

14 MeV Calibration of JET neutron detectors – Phase 2: in-vessel calibration

P. Batistoni^a, S. Popovichev^b, Z. Ghani^b, A. Cufar^c, L. Giacomelli^d, P. Hawkins^b, K. Keogh^b, S. Jednorog^e, E. Laszynska^e, S. Loreti^a, A. Peacock^g, M. Pillon^a, R. Price^b, A. Reed^b, D. Rigamonti^d, J. Stephens^b, J. Bielecki^f, S. Conroy^h, J. Dankowski^f, V. Krasilnikovⁱ and JET contributors¹

EUROfusion Consortium, Culham Science Centre, Abingdon, Oxon, OX14 3DB, UK

^a*ENEA, Department of Fusion and Nuclear Safety Technology, I-00044 Frascati (Rome), Italy*

^b*CCFE, Culham Science Centre, Abingdon, Oxon, OX14 3DB, UK*

^c*Reactor Physics Division, Jožef Stefan Institute, Jamova cesta 39, SI-1000 Ljubljana, Slovenia*

^d*Istituto di Fisica del Plasma “P. Caldirola”, CNR, Milano, Italy*

^e*Institute of Plasma Physics and Laser Microfusion, Hery 23, 01-497 Warsaw, Poland*

^f*Institute of Nuclear Physics Polish Academy of Sciences (IFJ PAN), PL-31-342 Krakow, Poland*

^g*JET Exploitation Unit, Abingdon, Oxon, OX14 3DB, UK / EC*

^h*Department of Physics and Astronomy, Uppsala University, Sweden*

ⁱ*ITER Organization, Route de Vinon-sur-Verdon, CS 90 046, St. Paul Lez Durance Cedex 13067, France*

Abstract

A new DT campaign (DTE2) is planned at JET in 2020 to minimize the risks of ITER operations. In view of DT operations, a calibration of the JET neutron monitors at 14 MeV neutron energy has been performed using a well calibrated 14-MeV neutron generator (NG) deployed, together with its power supply and control unit, inside the vacuum vessel by the JET remote handling system. The neutron generator was equipped with two calibrated diamond detectors, which continuously monitored its neutron emission rate during the calibration, and activation foils which provided the time integrated yield. Cables embedded in the remote handling boom were used to power the neutron generator, the active detectors and pre-amplifier, and to transport the detectors' signal. The monitoring activation foils were retrieved at the end of each day for decay γ -ray counting, and replaced by fresh ones. About 76 hours of irradiation, in 9 days, were needed with the neutron generator in 73 different poloidal and toroidal positions in order to calibrate the two neutron yield measuring systems available at JET, the ²³⁵U fission chambers (KN1) and the inner activation system (KN2). The NG neutron emission rates provided by the monitoring detectors were in agreement within 3-4%.

Neutronics calculations have been performed using MCNP code and a detailed model of JET to derive the response of the JET neutron detectors to DT plasma neutrons starting from the response to the NG neutrons, and taking into account the anisotropy of the neutron generator and all the calibration circumstances. These calculations have made use of a very detailed and validated geometrical description of the neutron generator and of the neutron source routine producing neutron energy-angle distribution for the neutron emitted by the neutron generator.

The KN1 calibration factor for a DT plasma has been determined with $\pm 4.2\%$ experimental uncertainty (1σ). It has been found that the difference between KN1 response to DD neutrons and that to DT neutrons is within the uncertainties in the derived responses. KN2 has been calibrated using the ⁹³Nb(n,2n)^{92m}Nb and ²⁷Al(n, α)²⁴Na activation reactions (energy thresholds 10 MeV and 5 MeV respectively). The total uncertainty on the calibration factors is $\pm 6\%$ for ⁹³Nb(n,2n)^{92m}Nb and $\pm 8\%$ ²⁷Al(n, α)²⁴Na (1σ). The calibration factors of the two independent systems KN1 and KN2 will be validated during DT operations.

The experience gained and the lessons learnt are presented and discussed in particular with regard to the 14 MeV neutron calibrations in ITER.

¹ See the author list of “X. Litaudon et al 2017 Nucl. Fusion 57 102001”

1. Introduction

JET is the largest fusion device in operation and the only one that can operate with tritium. A new DT campaign (DTE2) is planned at JET in 2020 to minimize the risks of ITER operations by testing strategies for the management of the in-vessel tritium content, investigating operational scenarios from non active operations to DT mixtures, and addressing the issue of neutron measurements accuracy and of neutron induced effects in materials. In view of DT operations, a calibration of the JET neutron monitors at 14 MeV neutron energy has been performed to allow the accurate measurement of the fusion power, to reduce the uncertainty margin on the neutrons produced as compared to the allowed neutron budget, and so maximize the scientific return on DTE2 investment. Moreover, the JET 14 MeV neutron calibration has also the objective to benchmark the ITER neutron calibration, where $\pm 10\%$ accuracy is required for tritium accountancy.

The JET neutron source intensity ranges from $\approx 10^8$ n/s in hydrogen and deuterium ohmic operations to nearly 10^{19} n/s in DT operations. The absolute neutron emission rate is measured over the whole variation range with different detector systems (Fig.1): (a) three pairs of $^{235}\text{U}/^{238}\text{U}$ fission chambers (KN1) mounted in moderator packages at mid-plane locations close to the transformer magnet limbs in Octants 2, 6 and 8, and (b) the in-vessel activation system (KN2) which pneumatically delivers and retrieves capsules containing activation foils to/from ‘Irradiation Ends’ located at the edge of the vacuum vessel. It is common practice to deliver capsules before a pulse and retrieve them immediately after the pulse for measuring the induced gamma activity in the foils to determine the neutron fluence and spectra at that point in the vessel. The subsequently activated material samples are measured on High Purity Germanium detectors (HPGe), on which the induced gamma ray spectrum is measured and reaction rates deduced.

KN2 and the three KN1 ^{235}U fission chambers were independently calibrated in 2013 at 2.5 MeV neutron energy for JET D plasma operations [1, 2] using a ^{252}Cf source (emitting neutrons with a mean energy of 2.1 MeV) deployed inside the vacuum vessel by the JET remote handling system. The source was located at different toroidal/poloidal locations inside the JET vacuum vessel to simulate the volume plasma source. After the calibration, the neutron yields from D plasmas measured by the four calibrated systems agreed within $\pm 3\%$, i.e. within the combined uncertainty of the different systems of $\sim 10\%$ [2].

For the 14 MeV neutron calibrations there are no naturally occurring neutron sources at the relevant energy that could be conveniently employed, and neutron generators have to be used. 14 MeV neutron calibrations have been previously performed in JET [3] and performed in TFTR [4], overall accuracies of $\pm 10.4\%$ and $\pm 13\%$ were estimated, respectively.

In the current 14 MeV calibration, a 14-MeV neutron generator is used and deployed inside the vacuum vessel by means of the remote handling system (RH), mounted on one of the two existing RH booms and its ‘MASCOT’(MANipolatore Servo COntrollato Transistorizzato) robotic arms which can bear a maximum weight of 10 kg. The constraints and early decisions which defined the main calibration approach, e.g., the RH compatibility and the limited space available, the technical requirements of the 14 MeV neutron generator and the deployment method and the safety and engineering aspects have been discussed in a separate paper [5]. As the neutron generator is not a stable neutron source, several monitoring detectors are attached to it by means of an *ad hoc* mechanical structure to continuously monitor the neutron emission rate and the total neutrons emitted during the in-vessel calibration.

The 14 MeV neutron generator type ING-17 (Fig.2) provided by VNIIA [6] was identified as a suitable source complying with the JET physical and technical requirements. The system consists of a Power Supply and Control Unit (PSCU) and a Neutron Generator (NG) connected by a power supply cable. The VHV (very high voltage) unit is enclosed within the NG, together with the sealed tube containing tritium and deuterium. One PSCU and two NGs were purchased because of the need to avoid delays in the JET programme in the case of a NG failure. They operate in continuous mode with a nominal neutron emission rate of 2×10^8 n/s. The neutron emitting tube size is 70 mm (diam) x 459 mm (length), and the total weight is

2.8 kg. The PSCU size is 356 mm x 315 mm x 110 mm and its weight is 4.6 kg. The main characteristics of the ING-17 neutron generators are given in [7,8,9].

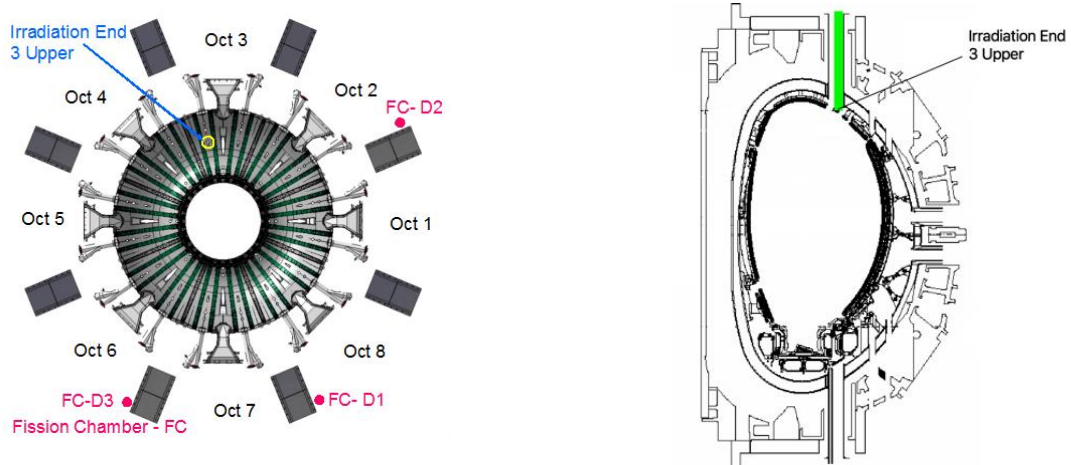


Fig.1 Left: Top view of JET machine showing the position of Fission Chambers (KN1) close to the magnetic limbs, and of the 3-Upper Irradiation End (KN2). Right: Cross section of JET showing the 3-Upper Irradiation End (KN2)

Their calibration and characterisation were achieved during two experimental campaigns at the National Physics Laboratory (NPL, Teddington, UK) from 9th to 20th November 2015 and from 13th to 17th June 2016 [10]. The results are summarised in the following:

- The neutron energy spectra of both NGs were measured in the energy range $E > 1.5$ MeV at different emission angles using a single crystal diamond and a NE213 liquid scintillator. The measured spectra could be very well reproduced by numerical simulation at all emission angles with a beam acceleration voltage of 73 keV, and with the beam composed of ~80.4% DT, ~8.95% D₂, 7.32% T₂, 2.66% T and ~0.63% D, and assuming that in the target there is the same mixture of deuterium and tritium [9,11].
- The anisotropy profile was measured for both NGs using absolutely calibrated long counters available at NPL, and with the relative emission rate provided by monitoring diamond detectors. The anisotropy profiles are identical for both NGs and could be very well produced by numerical simulations to within about $\pm 1\%$ [8].
- From the combined measurements of the long counters and monitoring diamond detectors, the total neutron emission in 4π sr was derived. It was about 2.6×10^8 s⁻¹ for NG#1 at the beginning, in agreement with the manufacturer's estimate, but it fell by about 25% during a shot near the end of the 2015 campaign. At the beginning of the 2015 campaign the total neutron emission of NG#2 was similar and dropped during the two campaigns but only about 12%. According to numerical calculations, these correspond to 1.012 times the neutrons produced in the target by fusion reactions due to interactions of neutrons with the NG body materials.
- The "monitoring diamond detectors" were calibrated against the long counters in terms of neutrons emitted by the NG per count within $\pm 3\%$.
- The absolute measurements of the neutron emission rates by the monitoring activation foils were found to be in agreement with those derived by the calibrated diamond detectors within 4%-5.8% and 4.0% for NG#1 and NG#2, respectively. The absolute measurements of the neutron emission rates by the NPL activation foils have been found to be in agreement with those derived by the calibrated diamond detectors within 2% and 4.6% for NG#1 and NG#2, respectively [12].
- The neutron source routine and the MCNP model of the NGs have been fully validated by the calibration/characterization measurements [7,8].

We concluded that, the absolute neutron emission rate during the JET in-vessel calibration could be derived from the diamond detectors with a total uncertainty equal to $\pm 3.1\%$ (uncertainty on absolutely calibrated neutron flux monitors used at NPL + uncertainty on diamond (n, α) peak count rate), and from monitoring activation measurements with a total uncertainty equal to $\pm 5.9\%$, provided that no other sources of uncertainties arise in the much more challenging environment due to the deployment of the NGs and their equipment by the RH system inside the JET torus. The neutron source routine and the MCNP model of the NGs can be reliably used in the analysis of the in-vessel calibration at JET.

At the end of the 2016 NPL campaign, the two neutron generators with the mechanical structures and all equipment were put back without any modification in their ad-hoc containers and stored ready for the in-vessel calibration at JET.

The present paper describes the outcome of the JET in-vessel calibration. The calibration factors for KN1 and KN2 have been derived with the related uncertainties and are presented. The final validation of the calibration and of the related accuracy will be obtained with measurements of neutron yields during DT operations, when the results obtained by the different calibrated detectors will be compared.

2. In-vessel calibration set up

The JET in-vessel calibration was performed from 28 January to 7 February 2017. NG#2 was chosen as it had the highest neutron emission rate at the end of the 2016 NPL campaign at about $2.4 \times 10^8 \text{ s}^{-1}$. The NG#2 was operated with the same assembly of mechanical structure, monitoring diamond detectors and activation foils, as used at NPL during the 2nd calibration/characterization campaign (Fig.2) in order to preserve the calibration factors obtained at NPL. Before the calibration commenced, the instrumentation package formed by the NG with the mechanical furniture, its Power Supply Control Unit (PSCU), the neutron monitoring detectors with amplifier and digitizer, and a laser based triangulation system, was commissioned in the Remote Handling (RH) construction workshop with similar lengths of fibres and data interface equipment to demonstrate all elements ‘worked’ correctly.

The whole instrumentation package was designed to be delivered into the vessel by the JET Octant 1 Boom (Fig. 3) and then assembled by the MASCOT, located at the end of the Octant 5 Boom, ‘on to itself’. The laser based triangulation system, was designed to ensure that the MASCOT could accurately position the NG at the desired distance from the in-vessel KN2 3-Upper irradiation end by observing the convergence of the two laser beams on the lower surface of the KN2 pocket. The only connectivity between the RH control room and the Torus Hall was via multi-mode optical fibres, with copper wire in the portion of the link bringing signals from the instrumentation down the boom before conversion to fibre. Temporary copper to fibre and fibre to copper media converters were installed to service these data links.

The campaign was preceded by about two weeks of testing and commissioning during the late shift with the NG and all instrumentation operated “as in vessel” in the Remote handling tent in Oct. 1 in the Torus Hall. After the first deployment, it was found that the power supply to the digitizer was ‘noisy’ to an unacceptable level. Noise on the DC supply caused the digitizer to add to the count of ‘genuine’ pulses from the neutron detectors. This was solved by changing the power supply type. Moreover, the data link to the digitizer was unreliable. Data could be logged from the digitizer for short periods, but the instrument would then go to ‘sleep’ and could not be ‘contacted’. The problem was solved by replacing the ‘USB over Ethernet’ by a small embedded computer (an Odroid XU4). After installation, the data link to the USB was robust and continued to function for the entirety of the calibration (see discussion in Section 6).

The in vessel calibration took 9 days of operations (two shifts per day) as planned. The NG#2 was operated in 227 shots in total (20 min each) for a total of 76 hours of irradiation. It remained very stable all along the campaign, with some more pronounced fluctuations only at the end. The calibration plan of measurements was fully completed. It must be noted that NG#2 had already operated for about 20 hours during the NPL campaigns.

For the calibration of KN1 fission chambers the NG#2 was located in 40 toroidal positions along a ring defined by the plasma toroidal axis (central ring, located at $R=300$ cm, $Z=30$ cm). The positions on the central ring were repeated a second time to evaluate the uncertainty in the positioning of the NG#2. Vertical and radial scans were performed as in the previous calibrations in Oct. 2, Oct. 6 and Oct. 8, as well as overlaps from vessel right and left in Oct.1 to investigate the effect of the presence of the MASCOT body on the fission chambers response.

For the KN2 Activation system irradiations were performed with the NG#2 in three irradiation positions selected based on duplicating the experimental set up used during the DD in-vessel calibration [1]. Irradiation times ranged from 3 hours (upper position) to 4.5 hours (lower position).



Fig. 2 – The Neutron Generator NG#2 on the left with the mechanical furniture supporting the monitoring diamond detectors and activation foils, and the box, to be attached to the MASCOT body, containing the PSCU, diamond detector digitizer, power supplies and the embedded computer emulating the ‘USB over Ethernet’ unit.



Fig. 3 – Calibration instrumentation package delivered in vessel by the JET Octant 1 Boom to be then seized by the MASCOT, located at the end of the Octant 5 Boom, and then assembled ‘on to itself’.

3. NG neutron yield measurement by monitoring diamond detectors and activation foils

The two diamond detectors were inserted in-vessel installed on the mechanical structure mounted on NG#2. The acquisition chain operated inside the vessel consisted of a CAEN preamplifier and a dual channel digitizer CAEN DT5780 which included the HV voltage source needed by the detectors. The system was remotely operated by the embedded computer emulating the ‘USB over Ethernet’ unit and

signals were transmitted through the copper wire embedded inside the remote handling boom. All the pulse height spectra (PHS) from the diamond detector signals were acquired in list mode so that post processing of data could be done.

One of the detectors (Dia#1) worked properly and with very high stability during all the 227 NG shots performed during the in-vessel campaign. The second detector (Dia#0) did not work properly all the time, probably due to an imperfect attachment of the diamond plate inside the casing nut. Nonetheless, data for about 130 shots are available for Dia#0.

After the elaboration of the first pulse height spectra it was discovered that it was not possible to use exactly the same setting used for the NPL calibration. In particular, the lower level threshold had to be increased due to the higher noise in the JET environment. However, it can be seen in Figs. 4-5 that the peak from the most important reaction used for detecting 14 MeV neutrons by the diamond detectors, the $^{12}\text{C}(n,\alpha)^9\text{Be}$ reaction, remained in the same position also after changing the lower energy threshold. Fig. 6 shows the comparison among three spectra and three $^{12}\text{C}(n,\alpha)^9\text{Be}$ peaks with different lower level threshold for different shots at the beginning, middle and at the end of JET campaign, normalized to peak area for Dia#1. It can be seen that the shape and position of the peaks remain unaffected by the change in the acquisition parameter along the JET campaign indicating also a very good stability of the whole electronic acquisition system. Thus, the calibration value obtained at NPL using the $^{12}\text{C}(n,\alpha)^9\text{Be}$ peak counts could be applied.

However, it can also be seen in Fig.4 and in Fig.5 that the relative efficiency of Dia#0 and Dia#1 changed as compared to the NPL campaign. The count rate of the initial shots at JET are shown in Fig.7 for both Dia#0 and Dia#1 in comparison with the count rates measured at NPL in the second campaign in 2016: the count rate of Dia#0 is almost unchanged at JET as compared to NPL (+4%) in the first 10 shots, and then an adjustment is observed to a count rate about 11% lower than at NPL 2016. This behavior, i.e. a temporary slight increase and then an adjustment after a few shots at the re-start of NG operation, had been observed previously during the NPL campaigns. On the other hand, the count rate of Dia#1 is higher by about 13% at JET as compared to NPL in the first 10 shots, and then an adjustment is observed to a count rate about 1.5% lower than at NPL, which is unrealistic considering that a reduction of at least of 3.5% is to be expected only due to tritium decay (from 17 June 2016 to 28 January 2017). Therefore, it appears that the efficiency of Dia#1 increased slightly as compared to NPL campaign.

The count rate obtained for all shots from Dia#1 and for the available shots for Dia#0 are shown in Fig.8 (Left). It can be seen that the neutron emission rate for the NG#2 is very stable after the initial drop at shot 11. Only after eight days of operation did the NG#2 yield decrease once more (shot190) and then remain stable until the end of the campaign.

The ratio of count rates of Dia#0 over Dia#1 is shown in Fig.8 (Right). It is 1.0715 ± 0.0178 ($\pm 1.663\%$) to be compared with 1.1732 ± 0.0027 obtained at NPL for NG#2. The ratio changed by about 10% and, considering the discussion above, the change appears to be due to Dia#1.

The total neutron yield for all shots can be obtained from the Dia#1 count rate multiplied by the factor obtained by cross calibration with Dia#0, i.e. 1.0715 ± 0.0178 ($\pm 1.663\%$). Fig.9 shows the total neutron yield of NG#2 during the JET in-vessel campaign as measured by calibrated diamond detectors. The total uncertainty includes the uncertainty on the cross-calibration factor ($\pm 1.663\%$), the uncertainty on the Dia#0 calibration obtained at NPL ($\pm 3\%$) [10], and the typical statistical uncertainty ($\pm 0.75\%$) yielding a total of $\pm 3.5\%$.

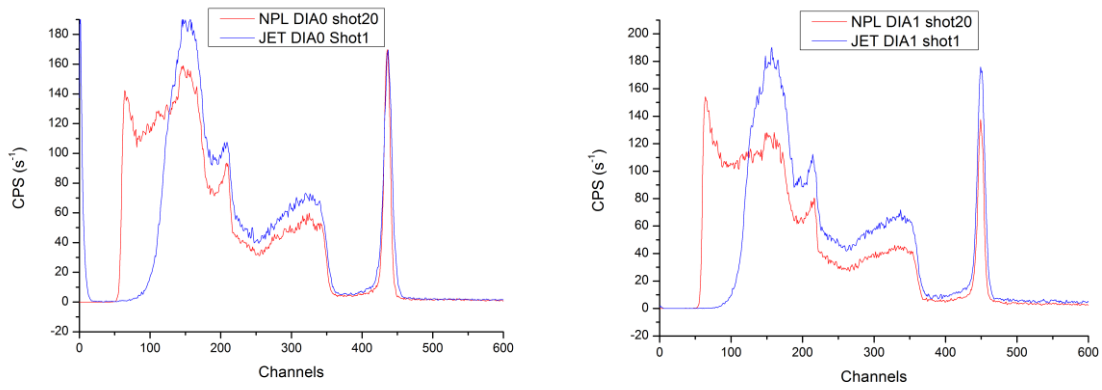


Fig.4 Comparison of count rates (CPS) in Dia#0 (left) and Dia#1(right) Pulse Height Spectra at the end of NPL campaign and at the beginning of the JET in-vessel campaigns

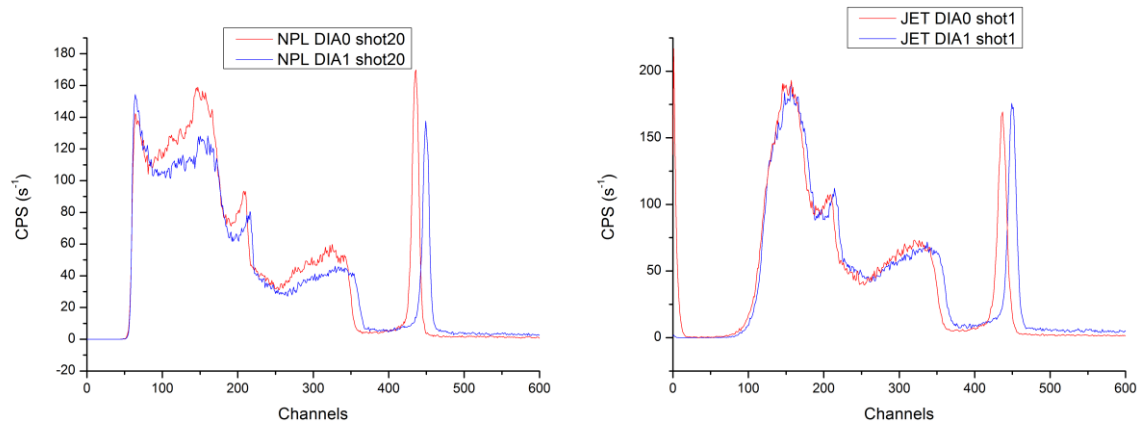


Fig.5 Comparison of count rates (CPS) in Pulse Height Spectra for Dia#0 and Dia#1 at the end of NPL campaign (left) and at the beginning of JET in-vessel campaigns (right).

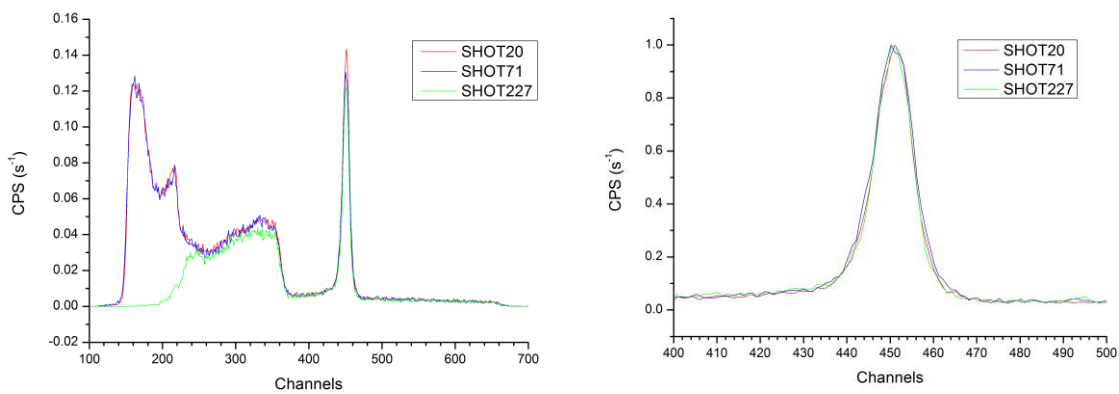


Fig.6 Comparison among three Pulse Height Spectra with different lower level threshold with Dia#1 during the JET campaign (left). Detail of the three $^{12}\text{C}(n,\alpha)^9\text{Be}$ peaks for the same Pulse Height Spectra, now normalized to peak area (right).

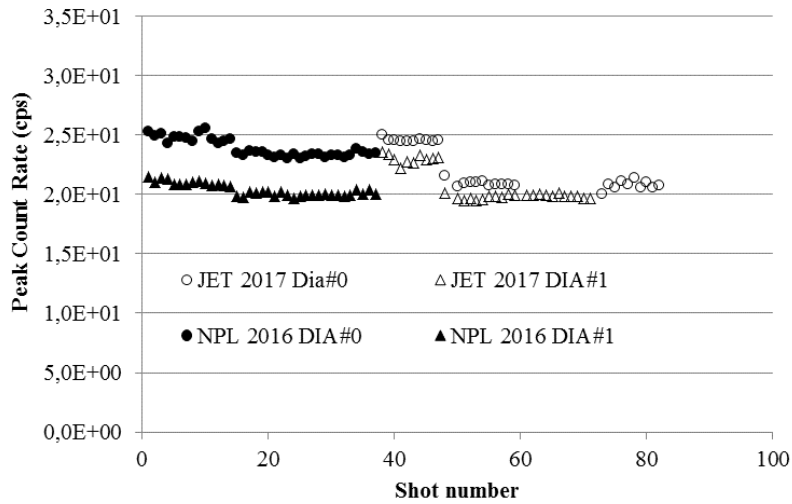


Fig.7 Count rates of the initial shots at JET for both Dia#0 and Dia#1 in comparison with the count rates measured at NPL in the second campaign in June 2016

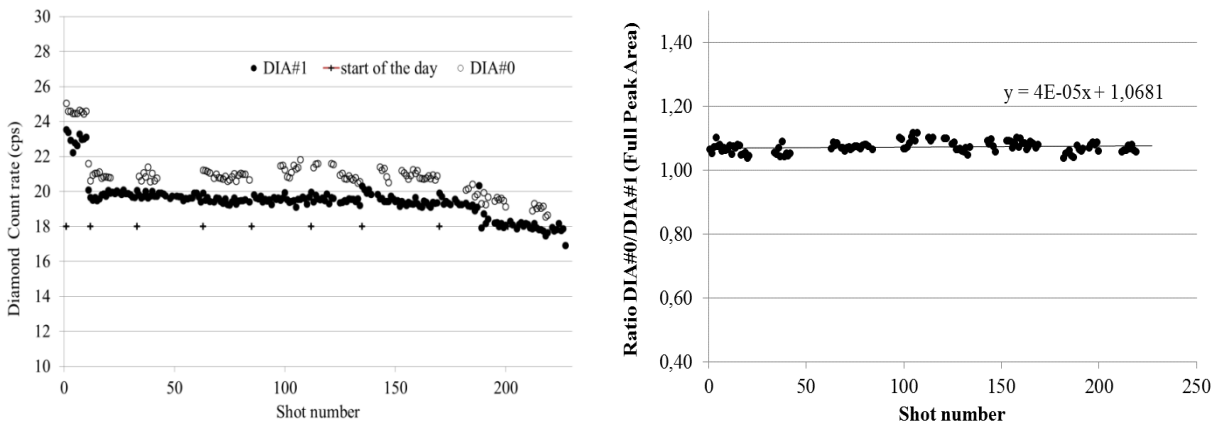


Fig.8 Count rates obtained from Dia#0 and from Dia#1 during the JET in vessel campaign (Left). Ratio of Dia#0 count rates over Dia#1 count rates (Right).

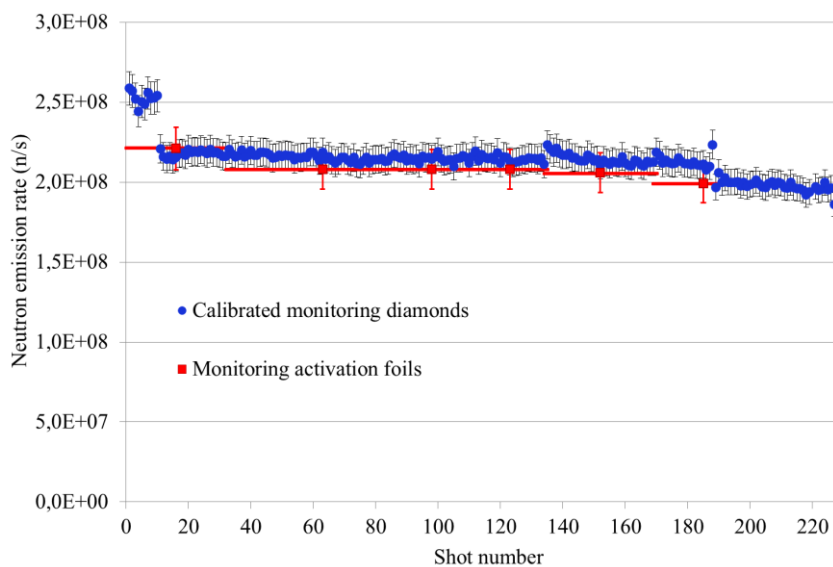


Fig. 9 – Total neutron yield of NG#2 during the JET in-vessel campaign as measured by calibrated diamond detectors (blue points). The red segments show the average neutron yields as independently measured by the activation foils on days 1-2, 3-4, 5, 6, 7 and 8. The agreement between the two methods is within about 3%.

The monitoring activation foils were removed from the mechanical support attached to NG#2 at the end of every calibration day and fresh foils were installed for the following day. The same activation reactions used during the NG calibration at NPL were employed, namely: $^{56}\text{Fe}(n,p)^{56}\text{Mn}$, $^{27}\text{Al}(n,\alpha)^{24}\text{Na}$ and $^{93}\text{Nb}(n,2n)^{92m}\text{Nb}$ (Table 1). The induced activity in the foils used was then measured in KN2 laboratory using a High Purity Germanium (HPGe) – an ORTEC GEM series, 38% relative efficiency detector. The average neutron emission during the day from the NG#2 was then derived and was found to be constant at about $2.08 \cdot 10^8$ n/s except for the first and last day (Fig.10). The total uncertainty ranged from 4.7% (^{92m}Nb) to 6.9% (^{24}Na) (1σ). The standard deviation of results from the different reactions was $\sim \pm 1\%$. The red points in Fig. 9 show the neutron emission rate as independently measured by the activation foils by the IPPLM team. The agreement with the neutron emission rate derived from diamond detectors is within 3%.

Table 1 Dosimetry reactions selected for the “monitoring” activation measurements

Reaction	Energy threshold (MeV)	Cross section at E=14 MeV (b)	Half-life	Isotopic abundance	Gamma energy (keV)	Gamma decay probability
$^{56}\text{Fe}(n,p)^{56}\text{Mn}$	4	0.11	2.579 h	0.918	846.8	0.989
$^{27}\text{Al}(n,\alpha)^{24}\text{Na}$	5	0.12	14.997 h	1	1368.6	0.999
$^{93}\text{Nb}(n,2n)^{92m}\text{Nb}$	9	0.46	10.15 days	1	934.5	0.991

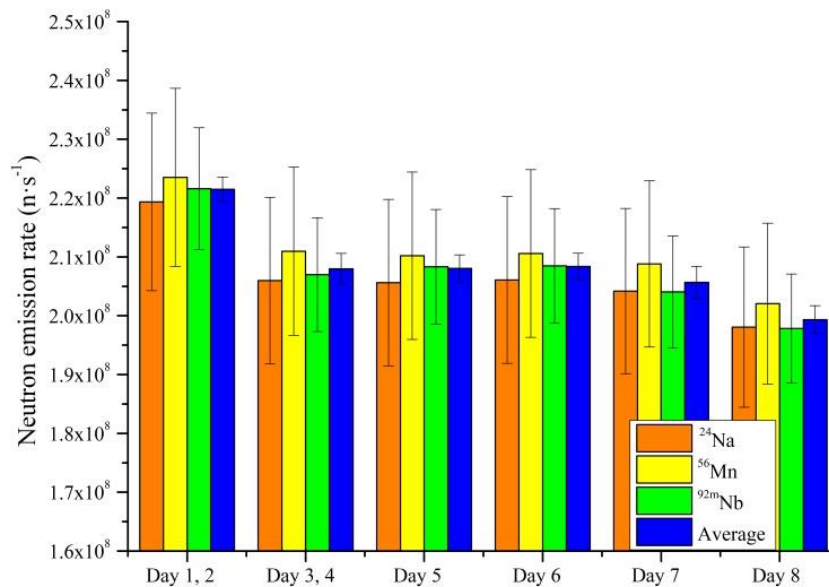


Fig. 10 Neutron emission rates derived from the activation measurements and average value (orange) for each day of in vessel calibration

4. KN1 Experiments

4.1 KN1 Measurements

As in the previous 2.5 MeV calibration in 2013, only the ^{235}U fission chambers have been calibrated. The ^{238}U fission chambers, which are used to extend KN1 dynamic range to high neutron emission rates in high performance DT pulses, have a lower efficiency (a factor of about 10000) as compared to the ^{235}U ones, which prevents their direct calibration with the typical intensity of the available portable neutron sources.

However, as the dynamic ranges of ^{235}U extends up to 10^{18} n/s and that of ^{238}U starts at $\sim 10^{17}$ n/s, they overlap in a sufficiently large range to allow a cross calibration of ^{238}U detectors [13].

In order to calibrate the ^{235}U fission chambers, the NG was located at 73 different poloidal and toroidal positions. It was located on 40 toroidal positions (Fig.11) along the plasma toroidal axis (central ring, located at $R=300$ cm, $Z=30$ cm) to simulate the extended plasma source, the same positions as for the 2.5 MeV calibration [1, 2]. No other off-axis rings were investigated, as previous calibrations proved that the plasma volume calibration function is very close to the calibration function obtained with the source on the central ring for realistic peaking factors of the plasma neutron emissivity profile [2]. The difference can therefore be easily evaluated by numerical simulations. The central ring positions were repeated a second time to assess the reproducibility of the measurement due to the uncertainty in the positioning of the NG. During the experiment, counting periods of 1200 s were used with the three FC's counting simultaneously.

As in the previous calibrations, port scans were also carried out at Octants 2, 6 and 8 with the source displaced from central positions (positions 6, 26 and 36, respectively, see Fig.11) by -50 cm, -25 cm, +25 cm and +50 cm both vertically and radially (note that the JET horizontal ports are centred at $Z=0$ and extend vertically from about $Z=-60$ cm to $Z=60$ cm).

Checks on the effect of the presence of the RH boom included the 'Overlap' measurements where the points around Octant 1 (3, 2, 1, 39, 40) were measured with clockwise (left) and anticlockwise (right) boom approach.

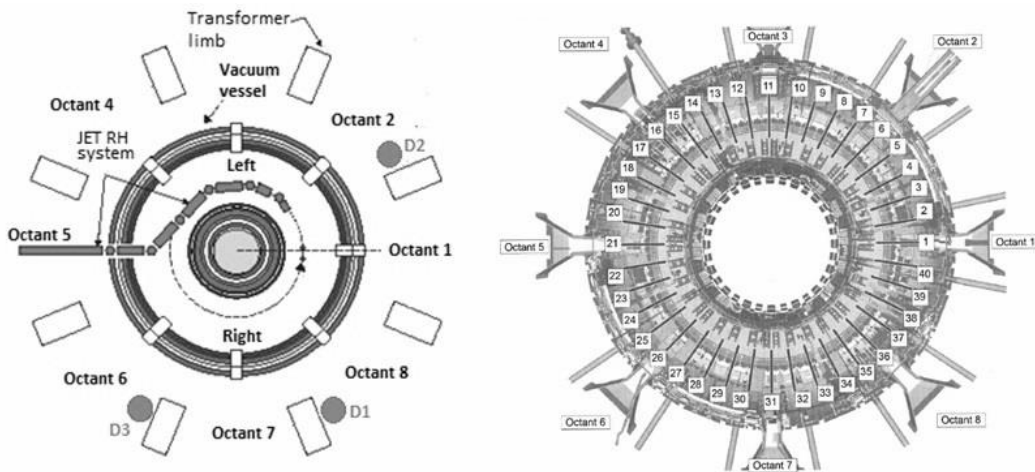


Fig.11 Sketch showing the position of the D1, D2 and D3 fission chambers and the RH boom deployment inside the JET torus (left). Neutron source positions for ring scan patterns in the JET torus (right)

The central ring data are summarised for all three detectors in Fig. 12. The integrals of the central rings data (first and second measurements) differ by less than 2% for all three detectors, showing the high reproducibility of the measurements. Note that no corrections have been applied to these data, apart from subtraction of the random backgrounds in the FCs and renormalization of the NG intensity (which varies shot by shot) to the intensity of the ^{252}Cf source, i.e. $2.62 \cdot 10^8$ n/s, which was used in the 2.5 MeV calibration in 2013. With this normalization, after the background subtraction, the total counts integrated over the central ring were 31665, 17280 and 33917 for D1, D2 and D3 respectively. The background amounted to 0.8%, 4.8% and 3.5%, respectively. The new NG data were compared with the ^{252}Cf calibration data, also shown in Fig. 12 (renormalised to 1200 s counting time). The shapes of each detector response to the NG source is very close to the response to the ^{252}Cf source, although some differences are observed: in Oct.2, where the variation is due to the completion of the installation of the ITER-like

Antenna in the main horizontal port, and in Oct. 6, where the difference may be due to the effect of the anisotropy of the NG emission (that has a minimum at 90° [10]) which is enhanced by the reduced angular view of the line of sight due to the narrow collimation provided by the two limiters closely set to the Oct.6 port.

The results of ‘Overlap’ measurements around Octant 1 are shown in Fig.13 together with the central ring data (for which positions 1-3 where obtained with left approach and 39-40 with right approach). The error bars represent the statistical uncertainty in the measurements. The new data are compared with the same data obtained during the ^{252}Cf calibration showing the same quantitative trend within the statistical uncertainty and taking into account the uncertainty on the positioning of the neutron source (± 2 cm). When the boom body is fully in front of the port and impedes the streaming of neutrons through it (positions 3 from right and 39 from left), the response of the closest detectors in Octants 2 and 8 is reduced. In the case of Octant 6 the boom body in positions 39 and 40 in the central ring has a right approach and shields neutrons emitted towards the detector.

The results of radial and vertical scan measurements in Octant 8 are shown in Fig.14 where R_w is the radius of the scattering centre at the port window in the octant where the detector is located. $C_{point} \cdot X^2 = C_{point}(R_w^2 + R^2 - 2R_w R \cos \theta + Z^2)$, with $R = 300$ cm and $Z = 30$ cm, is the square of the distance between the point of emission and the port scattering centre multiplied by the measured counts normalized to the intensity of the ^{252}Cf source used in 2013 calibration [2]. Following the analysis developed in [2], we observe that $C_{point} \cdot X^2$ remains approximately constant over the vertical point scan with a value of the radius if the scattering centre equal to $R_{w,v} = 470$ cm, as was found in the Cf calibration. This is true also for the radial scan: $C_{point} \cdot X^2$ are approximately constant across the scan for a value of the radius if the scattering centre equal to $R_{w,r} = 618$ cm as found for the ^{252}Cf calibration, with the exception of the innermost positions where the backscattering from the MASCOT body is larger due to it being in a closer position as compared to the ^{252}Cf case.

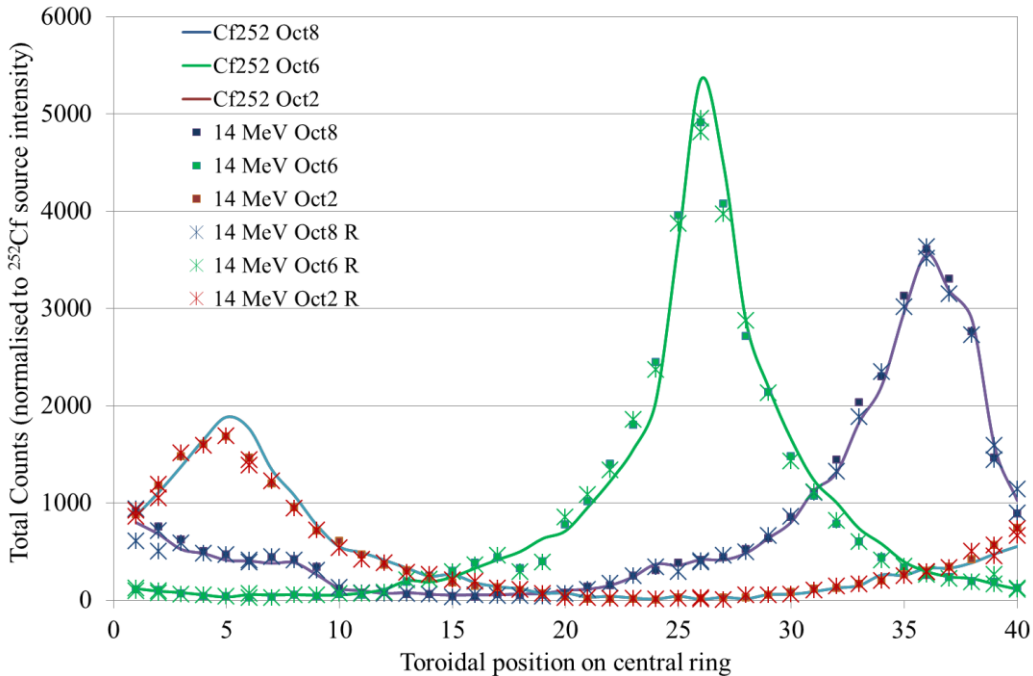


Fig. 12 Fission chambers central ring data (squares) for all three detectors, all normalized to a source intensity of $2.62 \cdot 10^8$ n/s. The stars represent the second collection of central ring data (Repeat). The continuous lines show the response curves measured in 2013 during the 2.5 MeV calibration using a ^{252}Cf source of intensity $2.62 \cdot 10^8$ n/s (normalised to 1200 s counting time per shot).

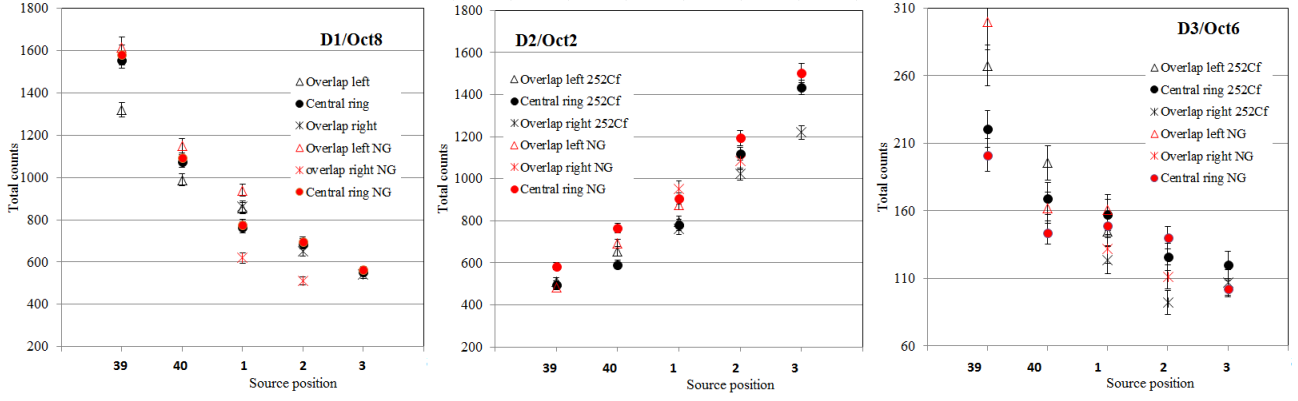


Fig.13 Overlap data around Octant 8 and data taken in the central ring scan for the three fission chambers in the case of NG source, and in the case of the ^{252}Cf source for comparison, all normalized to a source intensity of $2.62 \cdot 10^8$ n/s.

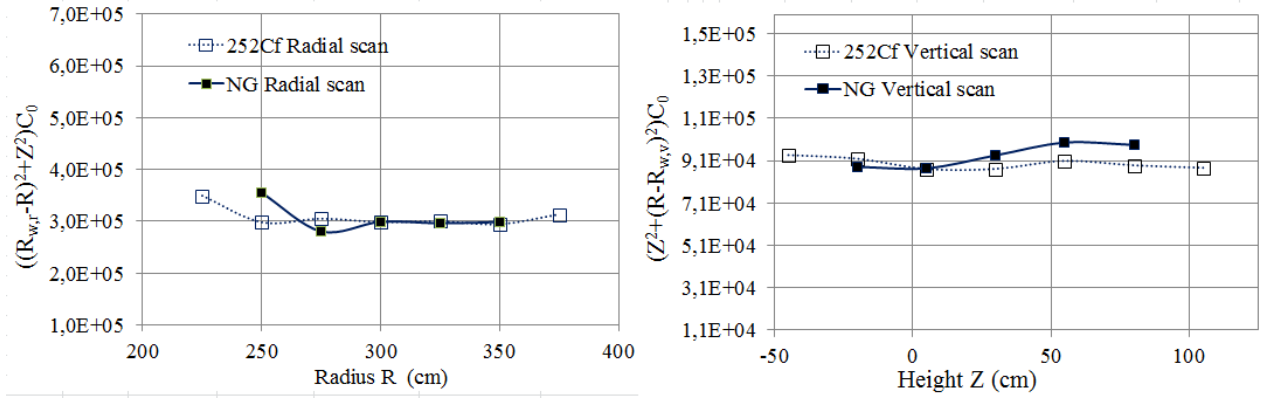


Fig.14 Radial (left) and vertical (right) scan data in Octant 8 in the case of NG source, and in the case of the ^{252}Cf source for comparison, all normalized to a source intensity of $2.62 \cdot 10^8$ n/s.

4.2 KN1 measurements analysis

Extensive MCNP calculations have been carried out to derive the KN1 calibration factors for DT plasmas. These calculations are needed to take into account the calibration circumstances, i.e. the use of a point source with given characteristics and the presence of the remote handling (RH) boom and MASCOT, which introduce differences as compared to plasma operation conditions.

First, the $R_{\text{NG+RH}}$ responses of KN1 fission chambers were calculated for all experimental configurations using the MCNP model of the NG and the source routine, both well validated in NPL campaigns [7,8,10], together with the MCNP model of the JET device, remote handling system and Torus Hall (Fig. 15). FENDL3.1b neutron transport cross-sections were used. The JET remote handling system is described using simple shapes, such as boxes and cylinders to explicitly model the casing of the RH system components which contain most of the mass [14,15]. However, the interior was modelled as a homogenous mixture of Al, Fe and Cu materials representing the electro-motors, stainless steel for wires, cables, W for balance weights. Any configuration of the JET RH system is defined by 21 coordinates, 9 defining one translation and eight rotations of the boom sections, and 12 defining the rotations of the joints (6 for each of the two arms). The modelling of the RH body in all experimental positions was achieved by an automatic MCNP input generation using FORTRAN scripts to translate RH configuration files to MCNP transformation cards.

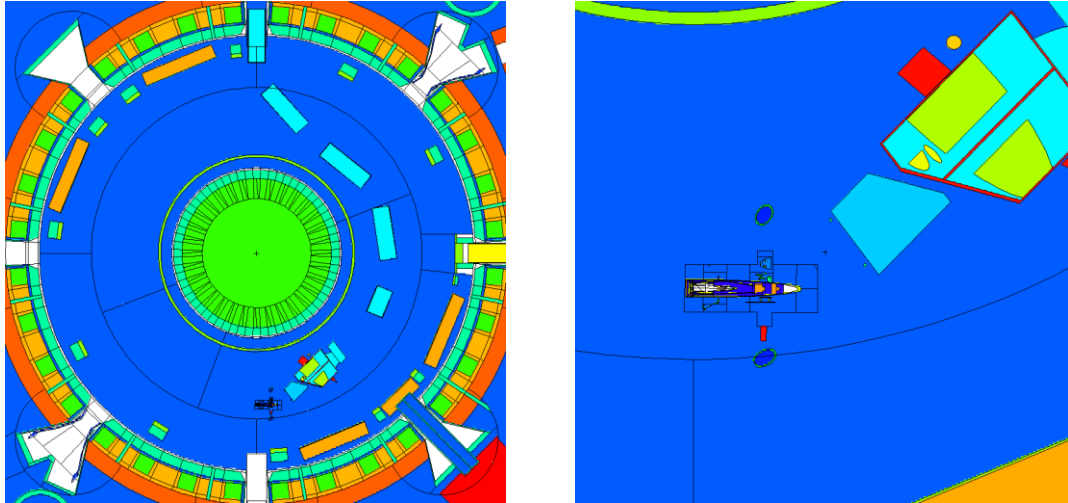


Fig. 15 Horizontal cross sections of the detailed MCNP model of JET with MASCOT boom deploying the NG inside the vessel (left). Detail of the model showing the NG (right)

Then the same KN1 responses were calculated for a point isotropic DT neutron source with Gaussian spectrum ($T=20$ keV) on the central ring with no presence of the RH system ($R_{DT,point}$). The comparison of $R_{NG+RH,point}$ and of $R_{DT,point}$ is shown in Fig. 16. In some positions the calculated correction factors for the effect of the NG anisotropy and RH system on the detector response are substantial. However, due to the low detector response at those positions, the global corrections for ring integrals are lower, ranging from 7% to 19% (Correction $R_{DT,ring}/R_{NG+RH,ring}$ in Table 2).

Finally, the same responses were calculated for the case of a DT plasma ($R_{DT,plasma}$). The plasma source used was constructed from 387 toroidal rings each with a square cross section of 10×10 cm. The emissivity assigned to each ring corresponds to a H-mode plasma emissivity with centre at $R=310$, $Z=30$ cm. The neutron energy spectrum was Gaussian with $T=20$ keV. The correction due to the shape of the neutron source is $\leq 2\%$, as already found in the analysis of the ^{252}Cf calibration (Correction $R_{DT,plasma}/R_{DT,ring}$ in Table 2).

The correction factors reported in Table 2 are applied to the experimental responses of FCs in the calibration measurements. The resulting calibration factors for DT plasmas for D1 (Oct.8), D2 (Oct.2) and D3 (Oct. 6) are shown in Table 2. The total uncertainty is estimated to be $\pm 4.2\%$, including the NG source intensity $\pm 3.5\%$, FCs counting statistics $< \pm 0.8\%$, NG positioning $< \pm 2\%$. Systematic errors in the simulations, due to approximations in the modelling of ports and of surrounding objects, are difficult to estimate and are not included. However, the results of the previous calibration in 2013 have demonstrated that the uncertainty on the correction factors due to modelling should be small.

Table 2 shows also the KN1 calibration factors obtained at the end of the ^{252}Cf calibration in 2013 for comparison. Immediately after the calibration, the neutron yields from DD plasmas measured by the three FCs and the activation system agreed within $\pm 3\%$. In the following years, however, modifications occurring outside the machine and close to the FCs have caused changes in time of their calibration factors which needed to be “re-tuned” by cross comparison with KN2 (which is not sensitive to changes in the configuration outside the machine). In particular, the main change was observed for D2 in Octant 2 (see Table 2) following the completion of the installation of the ILA with the addition of massive components outside the horizontal port. In order to assess the difference between DT and DD neutrons, the new DT calibration factors (2017) have to be compared with the DD calibration factors in 2016, i.e. referring to the same machine status. It can be seen in Table 2 that the difference is within a few percent, within the total combined uncertainty of the two measurements.

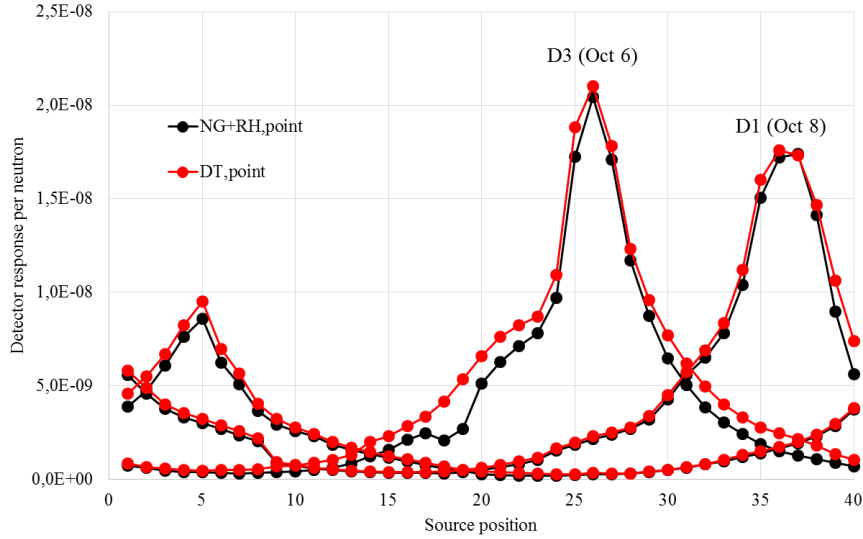


Fig. 16 Calculated response of fission chambers as a function of source position on the central ring for the real NG#2 calibration conditions ($R_{NG+RH,point}$) and for the case of an isotropic point DT source on the central ring without RH system ($R_{DT,point}$)

This result is explained by the slight decrease of the fission chamber response when moving from 2.5 to 14 MeV neutrons [16] (Fig.17), which is almost completely compensated for by the increased transparency of the JET machine components at higher neutron energy. This result has important consequences for operations with tritium with mixed 2.5 and 14 MeV neutrons as the KN1 calibration factor can be considered flat at these energies. The same conclusion applies for TT neutrons, which are emitted in an almost intermediate energy range, between 1 MeV and 9 MeV. This result allows also a direct discrimination of 14 MeV neutrons in operations with tritium, as KN1 always measures the total neutron yield (DD + TT + DT) whereas the 14 MeV neutrons can be discriminated by KN2 using suitable high threshold reactions (e.g. $^{93}\text{Nb}(n,2n)$).

Table 2 Summary of calculated (MCNP) correction factors for the KN1 FC calibration factors

	D1 / Oct 8	D2 / Oct 2	D3 / Oct 6
Integral of Central Ring (n/count) measured	$3.97 \cdot 10^8$	$7.28 \cdot 10^8$	$3.71 \cdot 10^8$
Correction $R_{DT,ring}/R_{NG+RH,ring}$	1.07	1.10	1.19
Correction $R_{DT,plasma}/R_{DT,ring}$	0.98	1.00	1.00
TOTAL Correction Factor	1.04	1.10	1.19
<i>DT plasma (n/count) (2017)</i>	$3.81 \cdot 10^8$	$6.61 \cdot 10^8$	$3.11 \cdot 10^8$
<i>DD plasma (n/count) (2014)</i>	$3.631 \cdot 10^8$	$5.261 \cdot 10^8$	$2.948 \cdot 10^8$
<i>DD plasma (n/count) (2016)</i>	$3.64 \cdot 10^8$	$6.98 \cdot 10^8$	$3.25 \cdot 10^8$
<i>DT(2017) / DD(2016)</i>	1.05	0.95	0.96

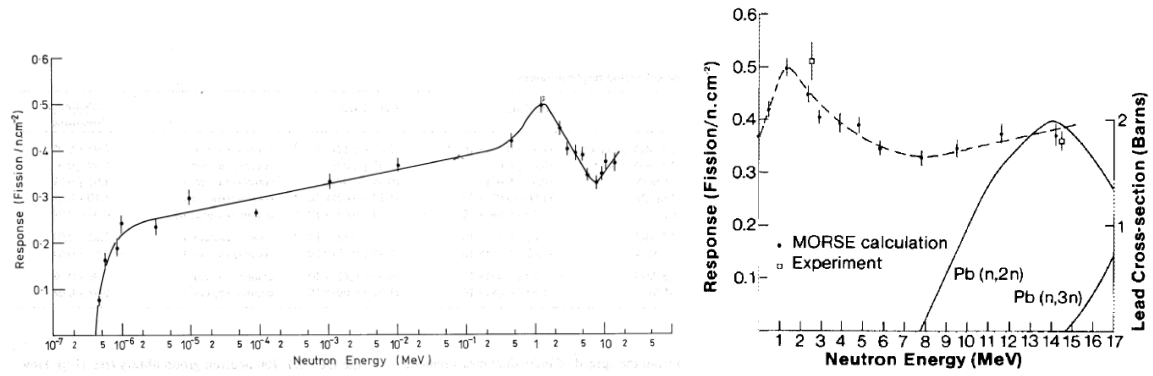


Fig. 17 Calculated and measured KN1 ^{235}U Fission chamber response on a logarithmic (left) and a linear energy scale (right) (from [16])

5 KN2 Experiments

In JET, the activation system is the reference system providing the absolute calibration for neutron yield measurements, due to its almost total insensitivity to changes in the machine external layout. The primary purpose of the KN2 diagnostic is to provide a reliable cross calibration of the KN1 time resolved neutron yield monitors.

5.1 KN2 Measurements

For the in-vessel calibration NG irradiations were carried out at three fixed positions relative to the KN2 activation end ‘3 upper (3U)’, located in Octant 3, this being the closest activation station to the vacuum vessel/plasma boundary and the one best characterised with both simulations and experiments.

The positions of these measurements were judiciously chosen such that the induced activity in activation foils in the 3U positions would be high enough to result in good gamma counting statistics when irradiation capsules are removed and that the NG fluence at this location would not be in a part of the NG angular distribution which is rapidly changing. The need for a flat neutron emission rate stems from that fact that the RH equipment can only position the NG to a positional uncertainty $\pm 1\text{cm}$ of the required position. An angle of 75 degrees was deemed suitable (Fig. 18) as the neutron emission rate approximately plateaus over a reasonable range of emissions angles, such that the difference in fluence ranging between 10 degrees of this angle differs by no more than 5%.

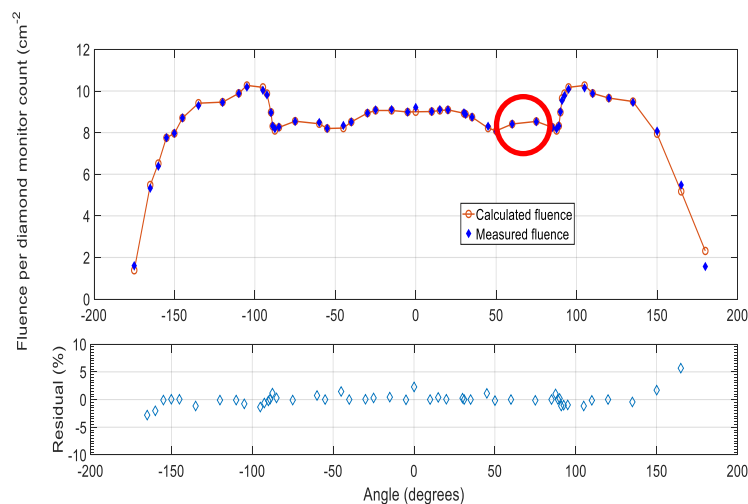


Fig.18 NG fluence angular distribution, the plateau in fluence is circled in red. The NG was positioned and orientated such that a cone with an opening angle of 75 degrees would intercept KN2 IE

Three irradiation positions were selected based on duplicating as far as possible the experimental set up used during the DD in vessel calibration [1]. These positions were:

- (i) 'Upper' position (at 33.9 cm distance from the irradiation end)
- (ii) 'Middle' position (at 52.1 cm distance from the irradiation end)
- (iii) 'Lower' position (at 66.9 cm distance from the irradiation end)

Activation foils were selected based on standard dosimetry requirements, including their high cross section to 14MeV neutrons and the availability of high quality processed nuclear data. Of the subset of foils selected Nb and Al were chosen to characterise the KN2 irradiation end. The KN2 pneumatic system has a mass limit of ~28 g when fully loaded. Nine KN2 irradiations were carried out during the in-vessel calibration, at the three vertical displacements above the midplane, i.e. three repeat irradiations per position, with typically 10-14 shots of ~1200s duration per measurement.

Four Nb foils (99.9% purity, thickness = 2 mm, diameter = 18 mm) and one Al foil (99.9% purity, thickness = 2 mm, diameter = 18 mm) were precisely weighed (+0.0001g), and sent through the KN2 pneumatic systems, with the NG positioned at one of the KN2 positions. Following irradiation, activation foils are retrieved and split such that the four Nb foils were measured on a very high efficiency HPGe detector (ORTEC model GEM-MX94100-108-LB-C-S), with relative efficiency of approximately 175% and an energy resolution of 2.1 keV. The four foils were counted in a rosette geometry i.e. the foils placed in the corners of a square foil positioning system/spacer. For each set of measurements, the single Al foil was measured on a second HPGe (Canberra model GC2018, Standard Electrode Coaxial Ge Detector - SEGe) with a relative efficiency of ~20% and a resolution of 1.8keV. All the detectors were cross calibrated against a third HPGe detector, an ORTEC ~40% efficiency detector, which was used for the monitoring of foils mounted on the NG horse-shoe holder.

The measured gamma spectra were corrected for foil self attenuation and off axis foil measurement geometry corrections as well as neutron yield variation during NG irradiation.

5.2 KN2 Measurement analyses

The induced activities were compared to calculated activities, using MCNP simulations with the exact foil stack being irradiated, NG and remote handling system included in the JET tokamak model.

Calculated to experimental ratios (C/E), weighted by measurement uncertainties, show an average weighted C/E of 0.974, 1.084 and 1.047 for upper, middle and lower positions respectively (Figure 19), resulting in a combined weighted C/E of 1.036 with a $\pm 5\%$ standard deviation. The weighted average of Nb and Al foils for a given irradiation favoured the more precise (less uncertain) Nb measurements ($\pm 6\%$ uncertainty) resulting in larger weight contributions to the total C/E calculation for these foils, versus the $\pm 8\%$ in the total measurement uncertainty on each Al foil.

The simulated reaction rates in the foils agree to within the respective uncertainties to the measured results, thus confirming the validity of computed DT calibration coefficients and further validating the MCNP model of KN2 for future cross calibrations between KN1 and the KN2 diagnostic.

Preliminary activation coefficients have been derived for DT plasmas, they are $2.66 \cdot 10^{-31}$ activated nuclei/(target nuclei·neutron) for Nb and $8.04 \cdot 10^{-31}$ activated nuclei/(target nuclei·neutron) for Al. These values, however, depend on the foil configuration and are derived for the configuration of foils adopted during the calibration.

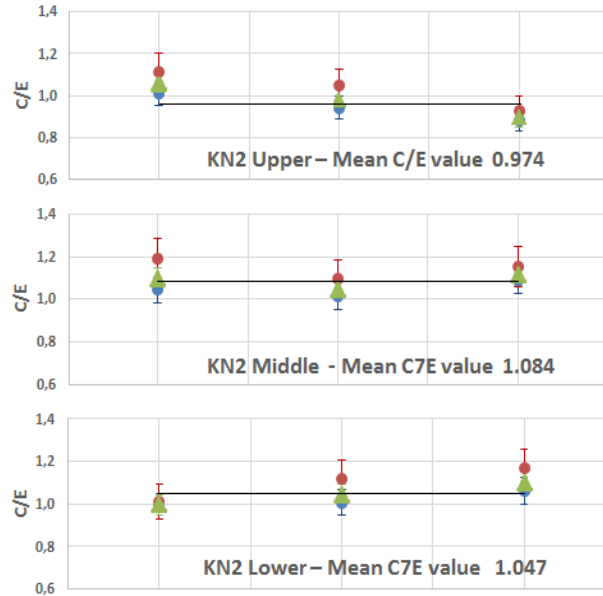


Fig.19 Calculated over measured (C/E) activities in Nb and Al foils. for upper, middle and lower positions respectively. The black lines indicate weighted average C/E value for each position.

6. Lessons learned and implications for ITER neutron calibration

The JET 14 MeV calibrations required the development of an original methodology for the characterization of the calibration source and for its deployment inside the JET vacuum vessel by means of the remote handling system. Several conclusions can be drawn, and important lessons were learned which provide valuable experience for future neutron calibrations in ITER and other fusion machines.

First of all, the mechanical furniture supporting the monitoring detectors was originally designed to be as light as possible in order not to perturb the spectrum of the emitted neutrons. As a consequence, it was not rigid enough which caused issues in obtaining a stable calibration of the monitoring detectors. This was partially improved after the first campaign at NPL when the front plate was changed to a plate with a hole rather than the open legs it originally was. However, the impact of the presence of the mechanical structure was proved to be minimal and it could have been more robust and stable. Issues with the furniture on the tube not allowing an accurate changing from NG#1 to NG#2 and viceversa resulted in the creation of a second set of furniture, but it would have been very useful to have also had a second pre-amplifier and a second set of monitoring diamond detectors.

Using different and independent detectors to monitor the NG emission rate was key for the success of the in-vessel calibration, and the achievement of the target accuracy. However, neither the detectors nor the NG were tested against mechanical shaking to verify that the mechanical assembly and contacts of active monitoring detectors were tested against mechanical robustness for deployment by the remote handling systems. Moreover, all electrical circuits were proven to work well in the NPL environment, but they turned out not to be reliable enough in the JET environment and had to be improved particularly with higher performance data links. Although the monitoring activation foils (passive detectors) introduced significant complication in the calibration plan, with changes and safety controls at the end of every day,

they provided a fundamental complementary and back-up system for monitoring the NGs in the in-vessel harsh conditions.

In ITER several neutron systems with different sensitivities are foreseen to measure ITER expected neutron emission from 10^{14} n/s up to almost 10^{21} n/s [17]. The measurement of total neutron emissivity is performed by means of neutron flux monitors. Unlike JET, many of ITER's monitors will be installed inside the vacuum vessel, aiming to decrease the effect of environment on the measurements. The Neutron Activation System (NAS), with irradiation ends inside the vacuum vessel, like in JET, will provide neutron yield data. Though there are differences between JET and ITER, the JET 2.5 and 14 MeV calibrations are very valuable experience for ITER. In fact, JET calibrations have proved the feasibility of

- accurate characterization of a 14 MeV neutron generator with intensity of $2.5 \cdot 10^8$ n/s, to be compared with $\geq 10^9$ needed in ITER,
- accurate calibration of active monitoring detectors providing the NG time resolved neutron emission rate,
- successful in-vessel operation of a NG with all instrumentation with remote handling system.

Based on the JET experience, it is recommended that in ITER

- the neutron calibration equipment and set up (neutron generator, monitoring detectors, power supply units, electronics and electrical connections and links) must be calibrated and tested on site under representative working conditions. Real working conditions should be simulated in advance as much as possible. Transporting the equipment or changing the working conditions may alter the calibration of monitoring detectors and then require time for remedial solutions during the in-vessel calibration;
- a neutron facility should be available on site in which it is possible to operate neutron sources, calibrate / re-calibrate detectors, test calibration equipment.

One concern in ITER is that the calibration of all systems may require a long time. The results obtained at JET show that central ring calibration scans and reference port scans are sufficient for fission chambers, and that a few calibration positions are sufficient to validate the neutronics models of activations systems. Neutronics analyses using state-of-art numerical tools can be applied with confidence provided that very accurate and detailed models are used in simulations. Moreover, the response function of active monitors (fission chambers) should be measured in advance and should be very well known. This will allow to complement direct calibration measurements (which could be limited in space due to time constraints) with numerical simulations which require the knowledge of the detector response function in the whole neutron energy range.

Finally, the activation system (at least a few selected Irradiation Ends) should be used as reference system for the absolute calibration of all monitors over the total neutron emission range;

Recently at JET a “long term irradiation station (LTIS)” has been also developed in which activation foils are irradiated for long periods (one or more experimental campaigns). After retrieval, the long decay time activity of the foils is measured from selected dosimetry reactions, providing the local neutron fluence at the LTIS [18]. From this the total neutron yield during the irradiation time can be derived using calculated reaction rates per source neutrons. The LTIS is located close to the first wall and its configuration is very simple, so that calculations of reaction rates do not introduce significant uncertainties especially when high energy threshold dosimetry reactions are used. It is proposed that ITER will consider the installation of similar dosimetry foils in reference positions on components inside the vessel which could be periodically removed and provide a periodic independent check of the neutron calibration.

7. Conclusions

The 14 MeV calibration of JET neutron monitors has been successfully achieved using a neutron generator deployed inside the JET vacuum vessel by the remote handling system. The 14 MeV neutron generator used had been very well characterized in advance, and equipped with calibrated monitoring detectors providing the instantaneous neutron emission rate within $\pm 3.5\%$ uncertainty. The calibration factors for DT plasmas have been obtained from direct measurements of the response function of JET neutron monitors with the required corrections provided by neutronics analyses. The accuracy achieved on the calibration

factors is well within the project target value ($\pm 10\%$), i.e. $\pm 5\%$ for the fission chambers (KN1) and $\pm 6\text{--}8\%$ for the activation system (KN2).

The difference between DT and DD calibration factors for KN1 was found to be small (within uncertainties), and so it is also deduced for TT calibration factors. Thanks to this result, in operations with TT plasmas (which also produce significant amounts of DT neutrons due to D contamination) KN1 can provide the total neutron yields whereas KN2 with Nb foils can provide the 14 MeV neutron yield. The 14 MeV calibration factors will be confirmed with DT plasmas when KN1 and KN2 will measure independently the same DT yield, provided no changes are made in the meantime around the fission chambers, which are very sensitive to variation in the machine configuration in the octant area where they are located.

The calibration methodology adopted for JET has been developed and implemented for the first time in a tokamak using state-of-art measurement and numerical techniques. The experience gained, and lessons learned, discussed in this paper, provide valuable experience for future neutron calibrations in ITER and other fusion machines.

Acknowledgements

This work has been carried out within the framework of the EUROfusion Consortium and has received funding from the Euratom research and training programme 2014-2018 under grant agreement No 633053. The views and opinions expressed herein do not necessarily reflect those of the European Commission.

References

- [1] D.B. Syme, S. Popovichev, S. Conroy, I. Lengar, L. Snoj, C. Sowden, L. Giacomelli, G. Hermon, P. Allan, P. Macheta, D. Plummer, J. Stephens, P. Batistoni, R. Prokopowicz, S. Jednorog, M.R. Abhangi, R. Makwana, Fusion yield measurements on JET and their calibration, *Fusion Engineering and Design* 89 (2014) 2766–2775
- [2] P. Batistoni, S. Popovichev, S. Conroy, I. Lengar, A. Čufar, M. Abhangi, L. Snoj, L. Horton and JET contributors, Calibration of JET neutron detectors, submitted to *Review of Scientific Instruments* (June 2017)
- [3] O. N. Jarvis, J. Kallne, G. Sadler, P. van Belle et al., Further calibrations of time-resolved neutron yield monitor (KN1), JET Joint Undertaking Internal Report JET-IR(85)06, 1985
- [4] D. L. Jassby, C. W. Barnes, L. C. Johnson, A. L. Roquemore, J. D. Strachan, D. W. Johnson, S. S. Medley, K. M. Young, Absolute Calibration of TFTF Neutron Detectors for DT Plasma Operation, Princeton Plasma Physics Laboratory Report, 1994
- [5] P. Batistoni, S. Popovichev, R. Crowe, A. Cufar, Z. Ghani, K. Keogh, A. Peacock, R. Price, A. Baranov, S. Korotkov, P. Lykin, A. Samoshin, Technical preparations for the in-vessel 14 MeV neutron calibration at JET, accepted or publication in *Fusion Engineering Design*
- [6] www.vniia.ru
- [7] A. Čufar, P. Batistoni, S. Conroy, Z. Ghani, I. Lengar, A. Milocco, L. Packer, M. Pillon, S. Popovichev, L. Snoj, Calculations to support JET neutron yield calibration: Modelling of neutron emission from a compact DT neutron generator, submitted to *Nuclear Instruments and Methods in Physics Research Section A*, 2016
- [8] Z. Ghani, S. Popovichev, P. Batistoni, S. Lilley, L. W. Packer, A. Milocco, A. Cufar, D. Plummer, D.J. Thomas, N.J. Roberts, L. Snoj, S. Jednorog, E. Laszyska, A. Peacock and JET contributors, Characterisation of a Neutron Generator and Monitoring Detectors, to be used for the in Vessel Calibration of JET, submitted to *Fusion Engineering and Design*
- [9] D. Rigamonti, L. Giacomelli, G. Gorini, M. Nocente, M. Rebai, M. Tardocchi, P. Batistoni, A. Cufar, M. Pillon, S. Loreti, M. Angelone, S. Popovichev, Z. Ghani et al, “ Neutron spectroscopy measurements of 14 MeV neutrons at unprecedented energy resolution and implications for deuterium–tritium fusion plasma diagnostics”, *2018 Meas. Sci. Technol.* 29 045502
- [10] P. Batistoni, S. Popovichev, A. Cufar, Z. Ghani, L. Giacomelli, S. Jednorog, A. Klis, S. Lilley, E. Laszyska, S. Loreti, L. Packer, A. Peacock, M. Pillon, R. Price, M. Rebai, D. Rigamonti, N. Roberts, M. Tardocchi, D. Thomas, 14 MeV calibration of JET neutron detectors—phase 1: calibration and characterization of the neutron source, *Nucl. Fusion* 58 (2018) 026012
- [11] A. Čufar, P. Batistoni, Z. Ghani, L. Giacomelli, I. Lengar, S. Loreti, A. Milocco, S. Popovichev, M. Pillon, D. Rigamonti, M. Rebai, M. Tardocchi, L. Snoj, Modelling of the Neutron Production in a Mixed Beam DT Neutron Generator, Submitted to *Fus. Eng. Design*

- [12] S. Jednorog, E. Laszynska, P. Batistoni, B. Bienkowska, A. Cufar, Z. Ghani, L. Giacomelli, A. Klix, S. Loreti, K. Mikszuta, L. Packer, A. Peacock, M. Pillon, S. Popovichev, M. Rebai, D. Rigamonti, N. Roberts, M. Tardocchi, D. Thomas, Activation measurements in support of the 14 MeV neutron calibration of 1 JET neutron monitors, submitted to Fusion Engineering Design
- [13] O. N. Jarvis, Treatment of the KN1 data channels, JET Report JET-TN (87)04, JET Joint Undertaking, Abingdon, Oxon, OX14 3EA, UK (1987)
- [14] L. Snoj, I. Lengar, A. Čufar, B. Syme, S. Popovichev, S. Conroy, L. Meredith, Calculations to support JET neutron yield calibration: Modelling of the JET remote handling system, Nuclear Engineering and Design, **261**, 2013, pp. 244-250.
- [15] L. Snoj, I. Lengar, A. Čufar, B. Syme, S. Popovichev, S. Conroy, L. Meredith, Modelling of the remote handling systems with MCNP - JET fusion reactor example case. V: Joint International conference on mathematics and computation (M&C), supercomputing in nuclear applications (SNA) and the Monte Carlo (MC) method, Joint International Conference on Mathematics and Computation (M&C), Supercomputing in Nuclear Applications (SNA) and the Monte Carlo (MC) Method, 19-23 April 2015, Nashville, 2015
- [16] M. T. Swinhoe, O. N. Jarvis, Calculation and Measurements of ^{235}U and ^{238}U fission counter assembly detection efficiency, Nuclear Instruments and Methods in Physics Research, 221 (1984) 460-465
- [17] L. Bertalot - Fusion Power Measurement at ITER - IEEE TRANSACTIONS ON NUCLEAR SCIENCE, VOL. 63, NO. 3, JUNE 2016
- [18] P. Batistoni, On the absolute calibration of neutron measurements in fusion reactors, Fusion Engineering and Design 105 (2016) 58-69